Arch Appl Mech (2008) 78: 105–116
DOI 10.1007/s00419-007-0145-x

ORIGINAL

B. Jin · Q. H. Fang

Piezoelectric screw dislocations interacting with a circular inclusion with imperfect interface

Received: 26 September 2006 / Accepted: 5 May 2007 / Published online: 6 June 2007

Abstract The electroelastic coupling interaction between multiple screw dislocations and a circular inclusion with an imperfect interface in a piezoelectric solid is investigated. The appointed screw dislocation may be located either outside or inside the inclusion and is subjected to a line charge and a line force at the core. The analytic solutions of electroelastic fields are obtained by means of the complex-variable method. With the aid of the generalized Peach–Koehler formula, the explicit expressions of image forces exerted on the piezoelectric screw dislocations are derived. The motion and the equilibrium position of the appointed screw dislocation near the circular interface are discussed for variable parameters (interface imperfection, material electroelastic mismatch, and dislocation position), and the influence of the nearby parallel screw dislocations is also considered. It is found that the piezoelectric screw dislocation is always attracted by the electromechanical imperfect interface. When the interface imperfection is strong, the impact of material electroelastic mismatch on the image force and the equilibrium position of the dislocation becomes weak. Additionally, the effect of the nearby dislocations on the mobility of the appointed dislocation is very important.

Keywords Screw dislocations · Imperfect interface · Piezoelectric solid · Image force

1 Introduction

The interaction between dislocations and other defects, such as cracks, cavities, and inclusions, plays an important role in understanding the physical behavior of many materials. The solution of the appropriate problem involving the interaction of dislocations with inclusions has two important physical interpretations. First, it increases the understanding of lattice defects, thereby providing valuable insight into the strengthening and hardening mechanism of materials [1–5]. Second, the solution of a single dislocation in solids can serve as the kernel function in an integral equation formulation for a crack, hole or finite defect [6,7].

As a typical intelligent material, piezoelectric materials are used widely in modern technologies such as high-power sonar transducers, electromechanical actuators, piezoelectric power supplies and micropositioners due to their useful electromechanical coupling effect. The presence of various defects embedded in piezoelectric materials, such as dislocations, cracks, cavities and inhomogeneities can greatly influence the performance of such piezoelectric devices and structures. A thorough understanding of the electroelastic coupling behavior of these devices requires accurate knowledge of both the electric and mechanical fields produced by these defects

B. Jin
College of Civil Engineering, Hunan University, Changsha, 410082, People's Republic of China

Q. H. Fang (✉)
College of Mechanics and Aerospace, Hunan University, Changsha, 410082, People's Republic of China
E-mail: fangqh1327@tom.com
Fax: +86-731-8822330

in piezoelectric materials. The investigation of the electroelastic interaction of dislocations and inclusions is thus significant [8–12].

In various studies [8–12] involving the electroelastic interaction of dislocations with inclusions in piezoelectric solids, the basic assumption was made that the bonding along the interface of two dissimilar materials is perfect. This is an idealization of the complex practical problem. In fact, this condition effectively ignores the presence of interfacial damage between the inclusion and the matrix, for example, damage arising from imperfect adhesions, microcracks, and microvoids. It was realized that the significance of damage or imperfection of the interface, in any mechanical analysis, is paramount in understanding the physical behavior of composite materials. One of most widely used models of an imperfect interface is based on the assumption that tractions are continuous but that displacements are discontinuous across the interface [13,14]. More precisely, jumps in the displacement components are assumed to be proportional, in terms of spring-factor-type interface parameters, to their respective interface traction components. Using this model (the spring-layer interface model), Fan and Wang [15], and Sudak [16,17] incorporated the effects of an imperfect interface into the analysis of a screw dislocation interacting with a circular inclusion. Recently, the problem of the interaction between an edge dislocation and a circular inclusion with imperfect interface was investigated by Wang [18].

In the present work, we consider the problem of the electroelastic interaction between multiple screw dislocations and a circular inclusion with an imperfect interface under anti-plane shear and in-plane electrical field loadings in a piezoelectric material. As regards the interface bonding imperfection, in addition to the spring-layer model adopted in the literature [14], we further employ a similar linear relationship between the discontinuities of electric potential and electric displacement [19]. By using the complex-variable method, the analytic solutions of electroelastic fields and image forces exerted on piezoelectric screw dislocations are derived. The impact of the interface imperfection, the material electroelastic mismatch, and the nearby dislocations on the image force acting on an appointed screw dislocation is examined and discussed when the dislocation is close to the inclusion.

2 Basic equations and solutions

Consider an infinitely long circular piezoelectric inclusion with a radius of R embedded in another piezoelectric matrix. The matrix and inclusion are assumed to be transversely isotropic media belonging to a hexagonal crystal class 6 mm with an isotropic basal xoy-plane in a Cartesian coordinate system xyz and have different elastic and electric properties, but they are assumed to have the same material orientation in that they have both been poled along the z-direction [20]. The matrix, assumed to be infinite in all directions, is subjected to remote uniform anti-plane shear stresses and in-plane electric fields. Several parallel piezoelectric screw dislocations are located at arbitrary points in either the matrix or the inclusion. Every screw dislocation is assumed to be straight and infinitely long in the z-direction, suffering a finite discontinuity in the displacement and electric potential across the slip plane and has a line force and a line charge along its core. The displacement jump across the slip plane corresponds to the Burgers vector, which is perpendicular to xoy-plane. The jump in the electric potential (the electric-potential dislocation) corresponds to the electric dipole layer along the slip plane [21,22]. The regions occupied by the inclusion and the matrix will be referred to as regions 1 and 2, respectively. The interface between the inclusion and the matrix is imperfect and will be denoted by the curve L. The imperfect interface is a mechanically compliant and dielectrically weakly conducting interface. For a mechanically compliant imperfect interface we adopt one of the more useful models, the linear spring model. For the case of a dielectrically weakly conducting interface, the normal electric displacement is continuous but the electric potential is discontinuous across the interface. Thus, the jump in the electric potential is proportional to the normal electric displacement [19].

As the current problem is an anti-plane one, the out-of-plane displacement and in-plane electric field need to be considered: the displacement w, the strains γ_{zx} and γ_{zy}, the stresses σ_{zx} and σ_{zy}, the electric potential φ, the electrical field components E_x and E_y, and the electric displacement components D_x and D_y in the local Cartesian coordinates. All components are only functions of x and y.

Introducing the following vectors of generalized displacement, stress and strain:

$$\mathbf{U} = \begin{Bmatrix} w \\ \varphi \end{Bmatrix}, \quad \Sigma_x = \begin{Bmatrix} \sigma_{zx} \\ D_x \end{Bmatrix}, \quad \Sigma_y = \begin{Bmatrix} \sigma_{zy} \\ D_y \end{Bmatrix}, \quad \mathbf{Y}_x = \begin{Bmatrix} \gamma_{zx} \\ -E_x \end{Bmatrix}, \quad \mathbf{Y}_y = \begin{Bmatrix} \gamma_{zy} \\ -E_y \end{Bmatrix} \tag{1}$$

Referring to work by Chen et al. [23], the generalized displacement, stress and strain can be expressed by a complex variable vector $\mathbf{f}(z) = \left[\, f_w(z)\ f_\varphi(z) \,\right]^{\mathrm{T}}$.

$$\mathbf{U} = \mathrm{Re}\,[\mathbf{f}(z)] \tag{2}$$

$$\mathbf{Y}_x - \imath\mathbf{Y}_y = \mathbf{f}'(z) \tag{3}$$

$$\Sigma_x - \imath\Sigma_y = \mathbf{M}\mathbf{f}'(z) \tag{4}$$

where the prime denotes the derivative with respect to the argument z and $\mathbf{M} = \begin{bmatrix} c_{44} & e_{15} \\ e_{15} & -\varepsilon_{11} \end{bmatrix}$ can be called the electroelasticity modulus matrix. And c_{44}, e_{15} and ε_{11} denote shear modulus, piezoelectric constant and dielectric constant of a piezoelectric solid, respectively. In terms of polar coordinates r and θ, Eq. (4) can be expressed as

$$\Sigma_r - i\,\Sigma_\theta = \mathbf{M}\mathbf{f}'(z)\mathrm{e}^{\imath\theta} \tag{5}$$

where $\Sigma_r = \left[\, \sigma_{zr}\ D_r \,\right]^{\mathrm{T}}$ and $\Sigma_\theta = \left[\, \sigma_{z\theta}\ D_\theta \,\right]^{\mathrm{T}}$.

Therefore, the resultant force and normal components of the electric displacement along any arbitrary arc AB is

$$\mathbf{T} = \int_A^B (\Sigma_x \mathrm{d}y - \Sigma_y \mathrm{d}x) = \mathbf{M}\,\mathrm{Im}\,[\mathbf{f}(z)]_A^B \tag{6}$$

It is prescribed that the circular inclusion is imperfectly bonded to the matrix along the L by the spring-layer interface model. The imperfect interface conditions on L are given by [14]

$$\mathbf{T}_2(t) - \mathrm{T}_1(t) = 0 \qquad |t| = R \tag{7}$$

$$\mathbf{U}_2(t) - \mathbf{U}_1(t) = \mathbf{Q}\Sigma_{r1}(t) = \mathbf{Q}\Sigma_{r2}(t) \qquad |t| = R \tag{8}$$

where the subscripts 1 and 2 refer to the inclusion and the matrix regions, respectively. $\mathbf{Q} = \begin{bmatrix} 1/K_\sigma & 0 \\ 0 & 1/K_e \end{bmatrix}$, K_σ denotes the bonding stiffness constant of the interface and K_e is the electric spring constant [19]. For a perfect bonded interface K_σ and K_e tend to infinity, while if $K_\sigma = K_e = 0$, condition (8) reduces to the case of a traction-free interface.

Firstly, let us consider the case of a single piezoelectric screw dislocation $\mathbf{b}_1 = \left[\, b_{z1}\ b_{\varphi 1} \,\right]^{\mathrm{T}}$ located at the point $z_1 (z_1 = x_1 + \imath y_1)$ in the matrix. The dislocation has a line force p_1 and a line charge q_1 along its core. The analytical function vector $\mathbf{f}_2(z)$ in the matrix region can be taken in the form

$$\mathbf{f}_2(z) = \mathbf{B}_1 \ln(z - z_1) + \Gamma z + \mathbf{f}_{20}(z) \qquad |z| > R \tag{9}$$

where $\mathbf{B}_1 = \frac{1}{2\pi i}\begin{bmatrix} b_{z1} \\ b_{\varphi 1} \end{bmatrix} + \frac{1}{2\pi}[\mathbf{M}_2]^{-1}\begin{bmatrix} -p_1 \\ q_1 \end{bmatrix}$ and $\mathbf{M}_2 = \begin{bmatrix} c_{44}^{(2)} & e_{15}^{(2)} \\ e_{15}^{(2)} & -\varepsilon_{11}^{(2)} \end{bmatrix}$ can be called the electroelasticity modulus matrix of the piezoelectric matrix material (region 2). Γ is determined by the remote shear stresses σ_{xz}^∞ and σ_{yz}^∞ and remote electric fields E_x^∞ and E_y^∞:

$$\Gamma = \frac{1}{c_{44}^{(2)}}\begin{bmatrix} 1 & -e_{15}^{(2)} \\ 0 & c_{44}^{(2)} \end{bmatrix}\begin{bmatrix} \sigma_{xz}^\infty - \imath\sigma_{yz}^\infty \\ -E_x^\infty + \imath E_y^\infty \end{bmatrix} \tag{10}$$

By applying the Riemann–Schwarz symmetry principle, two new complex potentials can be introduced

$$\mathbf{f}_{2*}(z) = \overline{\mathbf{f}_2}(R^2/z) \qquad |z| < R \tag{11}$$

$$\mathbf{f}_{1*}(z) = \overline{\mathbf{f}_1}(R^2/z) \qquad |z| > R \tag{12}$$

Using Eqs. (9) and (11), $\mathbf{f}_{2*}(z)$ can be expressed as

$$\mathbf{f}_{2*}(z) = \overline{\mathbf{B}_1}\ln\left(\frac{R^2}{z} - \overline{z_1}\right) + \overline{\Gamma}\frac{R^2}{z} + \mathbf{f}_{2*0}(z) \qquad |z| < R \tag{13}$$

where the overbar represents the complex conjugate.

Obviously, $\mathbf{f}_1(z)$ is holomorphic in the region $|z| < R$ if no singularities exist, and $\mathbf{f}_{1*}(z)$ is holomorphic in the region $|z| > R$.

With the aid of Eqs. (2), (5), (6), (11) and (12), the generalized traction and displacement boundary conditions in Eqs. (7) and (8) can be written as

$$[\mathbf{M}_1\mathbf{f}_1(t) + \mathbf{M}_2\mathbf{f}_{2*}(t)]^+ = [\mathbf{M}_2\mathbf{f}_2(t) + \mathbf{M}_1\mathbf{f}_{1*}(t)]^- \qquad |t| = R \tag{14}$$

$$\left[\mathbf{f}_1(t) - \mathbf{f}_{2*}(t) + \mathbf{Q}\mathbf{M}_1\mathbf{f'}_1(t)t/R\right]^+ = \left[\mathbf{f}_2(t) - \mathbf{f}_{1*}(t) + \mathbf{Q}\mathbf{M}_1\mathbf{f'}_{1*}(t)t/R\right]^- \qquad |t| = R \tag{15}$$

where the superscripts + and − denote the boundary values of a physical quantity as z approaches the interface.

Noting Eqs. (9–13) and according to the generalized Liouville theorem [24], Eqs. (14) and (15) lead to

$$\mathbf{h}(z) = \begin{cases} \mathbf{M}_1\mathbf{f}_1(z) + \mathbf{M}_2\mathbf{f}_{2*}(z) |z| < R \\ \mathbf{M}_2\mathbf{f}_2(z) + \mathbf{M}_1\mathbf{f}_{1*}(z) |z| > R \end{cases} \tag{16}$$

$$\mathbf{g}(z) = \begin{cases} \mathbf{f}_1(z) - \mathbf{f}_{2*}(z) + \mathbf{Q}\mathbf{M}_1\mathbf{f'}_1(z)z/R |z| < R \\ \mathbf{f}_2(z) - \mathbf{f}_{1*}(z) + \mathbf{Q}\mathbf{M}_1\mathbf{f'}_{1*}(z)z/R |z| > R \end{cases} \tag{17}$$

with

$$\mathbf{h}(z) = \mathbf{M}_2\mathbf{B}_1 \ln(z - z_1) + \mathbf{M}_2\overline{\mathbf{B}_1} \ln(\frac{R^2}{z} - \overline{z_1}) + \mathbf{M}_2\Gamma z + \mathbf{M}_2\overline{\Gamma}\frac{R^2}{z} \tag{18}$$

$$\mathbf{g}(z) = \mathbf{B}_1 \ln(z - z_1) - \overline{\mathbf{B}_1} \ln(\frac{R^2}{z} - \overline{z_1}) + \Gamma z - \overline{\Gamma}\frac{R^2}{z} \tag{19}$$

It is found from Eqs. (16) and (17) that

$$[\mathbf{M}_1 + \mathbf{M}_2]\mathbf{f}_1(z) + \mathbf{M}_2\mathbf{Q}\mathbf{M}_1\mathbf{f'}_1(z)z/R = \mathbf{M}_2\mathbf{g}(z) + \mathbf{h}(z) \tag{20}$$

The first differential equation above can easily be solved by the power-series method as [24]

$$\mathbf{f}_1(z) = \sum_{k=0}^{\infty} \mathbf{a}_k z^{k+1} \quad |z| < R \tag{21}$$

where

$$\mathbf{a}_0 = 2\left[\mathbf{M}_1 + \mathbf{M}_2 + \mathbf{M}_2\mathbf{Q}\mathbf{M}_1(1 + k)/R\right]^{-1}\mathbf{M}_2\left[\Gamma - \mathbf{B}_1(\frac{1}{z_1})\right] \tag{22}$$

$$\mathbf{a}_k = -2\left[\mathbf{M}_1 + \mathbf{M}_2 + \mathbf{M}_2\mathbf{Q}\mathbf{M}_1(1 + k)/R\right]^{-1}\mathbf{M}_2\mathbf{B}_1\frac{1}{1 + k}(\frac{1}{z_1})^{k+1} \quad k \geq 1 \tag{23}$$

From Eq. (12), it is seen that

$$\mathbf{f}_{1*}(z) = \sum_{k=0}^{\infty} \overline{\mathbf{a}_k} R^{2(1+k)} z^{-(k+1)} \tag{24}$$

The complex potential vector $\mathbf{f}_2(z)$ in the matrix region can be obtained from Eqs. (16) and (24).

$$\mathbf{f}_2(z) = \mathbf{B}_1 \ln(z - z_1) + \overline{\mathbf{B}_1} \ln\left(\frac{R^2}{z} - \overline{z_1}\right) + \Gamma z + \overline{\Gamma}\frac{R^2}{z} - \mathbf{M}_2^{-1}\mathbf{M}_1\sum_{k=0}^{\infty} \overline{\mathbf{a}_k} R^{2(1+k)} z^{-(k+1)} \tag{25}$$

In the absence of the piezoelectric coupling effect, the results of Eqs. (21) and (25) are identical to those of Sudak [16].

Secondly, as the counterpart problem, let us consider the case of a piezoelectric screw dislocation is inside the circular inclusion. The solutions valid for the dislocation located inside the inclusion could be used to

estimate the energy levels involved for a dislocation to cut the inclusion. For the problem under consideration, the complex potential vectors $\mathbf{f}_1(z)$ and $\mathbf{f}_2(z)$ can be taken in the form [25]

$$\mathbf{f}_1(z) = \mathbf{A}_1 \ln(z - z_1) + \mathbf{f}_{10}(z) \quad |z| < R \tag{26}$$

$$\mathbf{f}_2(z) = \mathbf{B}_1 \ln z + \mathbf{f}_{20}(z) \quad |z| > R \tag{27}$$

where $\mathbf{A}_1 = \frac{1}{2\pi i}\begin{bmatrix} b_{z1} \\ b_{\varphi 1} \end{bmatrix} + \frac{1}{2\pi}[\mathbf{M}_1]^{-1}\begin{bmatrix} -p_1 \\ q_1 \end{bmatrix}$. The complex function vectors $\mathbf{f}_{10}(z)$ and $\mathbf{f}_{20}(z)$ are holomorphic in the regions where they are defined.

The substitution of Eqs. (26) and (27) into Eqs. (11) and (12), respectively, leads to

$$\mathbf{f}_{1*}(z) = \overline{\mathbf{A}_1} \ln(z - \frac{R^2}{\overline{z_1}}) + \mathbf{f}_{1*0}(z) \quad |z| > R \tag{28}$$

$$\mathbf{f}_{2*}(z) = \overline{\mathbf{B}_1} \ln \frac{R^2}{z} + \mathbf{f}_{2*0}(z) \quad |z| < R \tag{29}$$

Similarly, the generalized traction and displacement boundary conditions in Eqs. (7) and (8) can be written as

$$[\mathbf{M}_1\mathbf{f}_1(t) + \mathbf{M}_2\mathbf{f}_{2*}(t)]^+ = [\mathbf{M}_2\mathbf{f}_2(t) + \mathbf{M}_1\mathbf{f}_{1*}(t)]^- \quad |t| = R \tag{30}$$

$$\left[\mathbf{f}_1(t) - \mathbf{f}_{2*}(t) + \mathbf{Q}\mathbf{M}_1\mathbf{f}'_1(t)t/R\right]^+ = \left[\mathbf{f}_2(t) - \mathbf{f}_{1*}(t) + \mathbf{Q}\mathbf{M}_1\mathbf{f}'_{1*}(t)t/R\right]^- \quad |t| = R \tag{31}$$

Noting Eqs. (26–29) and according to the generalized Liouville theorem [24], Eqs. (30) and (31) lead to

$$\mathbf{H}(z) = \begin{cases} \mathbf{M}_1\mathbf{f}_1(z) + \mathbf{M}_2\mathbf{f}_{2*}(z) & |z| < R \\ \mathbf{M}_2\mathbf{f}_2(z) + \mathbf{M}_1\mathbf{f}_{1*}(z) & |z| > R \end{cases} \tag{32}$$

$$\mathbf{G}(z) = \begin{cases} \mathbf{f}_1(z) - \mathbf{f}_{2*}(z) + \mathbf{Q}\mathbf{M}_1\mathbf{f}'_1(z)z/R & |z| < R \\ \mathbf{f}_2(z) - \mathbf{f}_{1*}(z) + \mathbf{Q}\mathbf{M}_1\mathbf{f}'_{1*}(z)z/R & |z| > R \end{cases} \tag{33}$$

with

$$\mathbf{H}(z) = \mathbf{M}_1\mathbf{A}_1 \ln(z - z_1) + \mathbf{M}_1\overline{\mathbf{A}_1} \ln\left(z - \frac{R^2}{\overline{z_1}}\right) - \mathbf{M}_2\overline{\mathbf{B}_1} \ln z \tag{34}$$

$$\mathbf{G}(z) = \mathbf{A}_1 \ln(z - z_1) - \overline{\mathbf{A}_1} \ln\left(z - \frac{R^2}{\overline{z_1}}\right) + \mathbf{Q}\mathbf{M}_1\mathbf{A}_1 \frac{z}{(z - z_1)R} + \mathbf{Q}\mathbf{M}_1\overline{\mathbf{A}_1} \frac{z}{(z - R^2/\overline{z_1})R} + \overline{\mathbf{B}_1} \ln z \tag{35}$$

From Eqs. (32) and (33) as well as Eq. (26), we have

$$[\mathbf{M}_1 + \mathbf{M}_2]\mathbf{f}_{10}(z) + \mathbf{M}_2\mathbf{Q}\mathbf{M}_1\mathbf{f}'_{10}(z)z/R = [\mathbf{M}_1 - \mathbf{M}_2]\overline{\mathbf{A}_1} \ln\left(z - \frac{R^2}{\overline{z_1}}\right) + \mathbf{M}_2\mathbf{Q}\mathbf{M}_1\overline{\mathbf{A}_1} \frac{z}{(z - R^2/\overline{z_1})R} \tag{36}$$

This equation can also be solved by the power-series method as

$$\mathbf{f}_{10}(z) = \sum_{k=0}^{\infty} \mathbf{b}_k z^{k+1} \tag{37}$$

where

$$\mathbf{b}_k = -\left[\mathbf{M}_1 + \mathbf{M}_2 + \mathbf{M}_2\mathbf{Q}\mathbf{M}_1(1 + k)/R\right]^{-1}\left[\mathbf{M}_1 - \mathbf{M}_2 + \mathbf{M}_2\mathbf{Q}\mathbf{M}_1(1 + k)/R\right]\overline{\mathbf{A}_1} \frac{1}{1 + k}\left(\frac{\overline{z_1}}{R^2}\right)^{k+1} \tag{38}$$

Therefore, the complex potential vectors $\mathbf{f}_1(z)$ and $\mathbf{f}_2(z)$ can be obtained as

$$\mathbf{f}_1(z) = \mathbf{A}_1 \ln(z - z_1) + \sum_{k=0}^{\infty} \mathbf{b}_k z^{k+1} \tag{39}$$

$$\mathbf{f}_2(z) = \mathbf{M}_2^{-1}\mathbf{M}_1\mathbf{A}_1 \ln(z - z_1) - \overline{\mathbf{B}_1} \ln z - \mathbf{M}_2^{-1}\mathbf{M}_1 \sum_{k=0}^{\infty} \overline{\mathbf{b}_k} R^{2(1+k)} z^{-(k+1)} \tag{40}$$

If we take $K_\sigma = K_e = \infty$ (for a perfect bonded interface), the solutions in Eqs. (39) and (40) are identical to the reduced results in Liu et al. [11].

The analytical solutions of the complex potential vectors have been given in Eqs. (21), (25), (39) and (41). The explicit solutions of electroelastic fields in the circular inclusion and the matrix regions can be easily derived from Eqs. (2–4).

Equations (21), (25), (39) and (41) are the explicit expressions of Green's functions for the current model subjected to a single piezoelectric screw dislocation located in either the matrix or the inclusion. The solutions for two or more screw dislocations in the matrix can be easily constructed by the superposition of Green's functions.

3 Image forces

The image force [26] on the dislocation is an important physical parameter in understanding the electroelastic behavior of inhomogeneous material, especially in studying the mobility and so-called trapping mechanism of the piezoelectric dislocation due to the fact that this mobility is dependent upon the internal forces acting on the dislocation. According to the generalized Peach–Koehler formula, the image force acting on a screw dislocation at the point z_1 can be obtained as [26]:

$$f_x - \imath f_y = \imath[b_{z1}, b_{\varphi 1}][\Sigma^0_{xj} - \imath\Sigma^0_{yj}] + [p_1, -q_1]\big[\mathrm{M}_j\big]^{-1}[\Sigma^0_{xj} - \imath\Sigma^0_{yj}] \quad (j = 1, 2) \tag{41}$$

where f_x and f_y are components of the image force along the x and y directions, respectively. Σ^0_x and Σ^0_y denote the perturbation generalized stress components at the point z_1.

The perturbation generalized stress components at the dislocation point are obtained by subtracting those attribution to the piezoelectric screw dislocation in the corresponding infinite homogeneous medium from the stress fields calculated using Eq. (4) for the current problem, then taking the limit for z approaches z_1. Referring to the work of Lee et al. [27], they can be written as

$$\Sigma^0_{x2} - \imath\Sigma^0_{y2} = \mathbf{M}_2\overline{\mathbf{B}_1}\left(\frac{1}{z_1 - R^2/\overline{z_1}} - \frac{1}{z_1}\right) + \mathbf{M}_2\Gamma - \mathbf{M}_2\overline{\Gamma}\frac{R^2}{z_1^2} + \mathbf{M}_1\sum_{k=0}^{\infty}\overline{\mathbf{a}_k}R^{2(1+k)}(1+k)(\frac{1}{z_1})^{k+2} \tag{42}$$

for the dislocation inside the matrix, and

$$\begin{aligned}\Sigma^0_{x1} - \imath\Sigma^0_{y1} = &-\mathbf{M}_1\sum_{k=0}^{\infty}\big[\mathbf{M}_1 + \mathbf{M}_2 + \mathbf{M}_2\mathbf{Q}\mathbf{M}_1(1+k)/R\big]^{-1} \\ &\times\big[\mathbf{M}_1 - \mathbf{M}_2 + \mathbf{M}_2\mathbf{Q}\mathbf{M}_1(1+k)/R\big]\overline{\mathbf{A}_1}(\frac{\overline{z_1}}{R^2})^{k+1}z_1^k\end{aligned} \tag{43}$$

for the dislocation inside the inclusion.

The image forces for the problem of multiple parallel screw dislocations located at arbitrary points in either the matrix or the inclusion phase can be derived by the superposition method. Consider the case that two parallel piezoelectric screw dislocations $\mathbf{B}_1$ and $\mathbf{B}_2$ are located at points z_1 and z_2 in the matrix, respectively. The total perturbation generalized stress components at the screw dislocation z_1 can be calculated as:

$$\begin{aligned}\Sigma^0_{x2} - \imath\Sigma^0_{y2} = &\mathbf{M}_2\overline{\mathbf{B}_1}\left(\frac{1}{z_1 - R^2/\overline{z_1}} - \frac{1}{z_1}\right) + \mathbf{M}_2\Gamma - \mathbf{M}_2\overline{\Gamma}\frac{R^2}{z^2} + \mathbf{M}_2\mathbf{B}_2\frac{1}{z_1 - z_2} + \mathbf{M}_2\overline{\mathbf{B}_2}\left(\frac{1}{z_1 - R^2/\overline{z_2}} - \frac{1}{z_2}\right) \\ &+2\mathbf{M}_1\sum_{k=0}^{\infty}\big[\mathbf{M}_1 + \mathbf{M}_2 + \mathbf{M}_2\mathbf{Q}\mathbf{M}_1(1+k)/R\big]^{-1}\mathbf{M}_2\left[\Gamma\delta_{0k} - \mathbf{B}_1(\frac{1}{\overline{z_1}})^{k+1}\right]\frac{R^{2(k+1)}}{z_1^{(k+2)}} \\ &-2\mathbf{M}_1\sum_{k=0}^{\infty}\big[\mathbf{M}_1 + \mathbf{M}_2 + \mathbf{M}_2\mathbf{Q}\mathbf{M}_1(1+k)/R\big]^{-1}\mathbf{M}_2\mathbf{B}_2(\frac{1}{\overline{z_2}})^{k+1}\frac{R^{2(k+1)}}{z_1^{(k+2)}}\end{aligned} \tag{44}$$

Similarly, for the case of two parallel piezoelectric screw dislocations $\mathbf{A}_1$ and $\mathbf{A}_2$ located at points z_1 and z_2 in the inclusion, respectively, we obtain

$$\begin{aligned}\Sigma_{x1}^0 - \imath\Sigma_{y1}^0 = &-\mathbf{M}_1\sum_{k=0}^{\infty}\left[\mathbf{M}_1+\mathbf{M}_2+\mathbf{M}_2\mathbf{Q}\mathbf{M}_1(1+k)/R\right]^{-1}\left[\mathbf{M}_1-\mathbf{M}_2+\mathbf{M}_2\mathbf{Q}\mathbf{M}_1(1+k)/R\right]\overline{\mathbf{A}_1}\left(\frac{\overline{z_1}}{R^2}\right)^{k+1}z_1^k\\ &+\mathbf{M}_1\mathbf{A}_2\frac{1}{z_1-z_2}-\mathbf{M}_1\sum_{k=0}^{\infty}\left[\mathbf{M}_1+\mathbf{M}_2+\mathbf{M}_2\mathbf{Q}\mathbf{M}_1(1+k)/R\right]^{-1}\\ &\times\left[\mathbf{M}_1-\mathbf{M}_2+\mathbf{M}_2\mathbf{Q}\mathbf{M}_1(1+k)/R\right]\overline{\mathbf{A}_2}\left(\frac{\overline{z_2}}{R^2}\right)^{k+1}z_1^k \qquad (45)\end{aligned}$$

Substituting Eqs. (42–45) into Eq. (41), the explicit expressions of the image force on the piezoelectric screw dislocation can be obtained for different cases. Here we omit the details to save space.

4 Results and discussion

Using the expressions of the image force given in Eq. (41), it is possible to discuss some characteristics of the problem under consideration. Firstly, we utilize Eq. (41) together with Eq. (42) to illustrate the influence of various parameters on the image force exerted on the dislocation when a single piezoelectric screw dislocation is located in the matrix. In the following discussion, without loss of generality, we suppose that the piezoelectric screw dislocation lies at the point x_1 on the x-axis. Additionally, we assume that the remote electroelastic loads vanish ($\Gamma = \mathbf{0}$) and that the line charge and line force are zero. In this case, $f_y = 0$ and the component of the normalized image force along the x-axis direction is defined as $f_{x0} = 2\pi R f_x/c_{44}^{(2)}b_{z1}^2$. Here, we take the piezoelectric screw dislocation vector $\mathbf{b}_1 = \left[\, b_{z1}\ b_{\varphi 1}\,\right]^{\mathrm{T}} = \left[\, 1.0\times10^{-9}m\ \ 1.0V\,\right]^{\mathrm{T}}$ and the piezoelectric matrix material is PZT-5H with the electroelastic properties: $c_{44}^{(2)} = 3.53\times10^{10}\mathrm{N/m^2}$, $e_{15}^{(2)} = 17.0\mathrm{C/m^2}$ and $\varepsilon_{11}^{(2)} = 1.51\times10^{-8}\mathrm{C^2/Nm^2}$ [28]. In addition, let us introduce four convenient nondimensional parameters: $m_1 = c_{44}^{(1)}/RK_\sigma$, $m_2 = e_{15}^{(1)}/RK_\sigma m_3 = e_{15}^{(1)}/RK_e$ and $m_4 = \varepsilon_{11}^{(1)}/RK_e$. Here, m_j ($j = 1, 2, 3, 4$) characterizes the effectiveness of bonding (degree of interface imperfection) at the interface in transferring load between the matrix and the inclusion. Physically, a very small value of m_j ($j = 1, 2, 3, 4$) corresponds to perfect bonding condition while a very large value of m_j ($j = 1, 2, 3, 4$) corresponds to a traction-free bonding condition.

Figures 1, 2, and 3 show the variation of the normalized force f_{x0} with respect to the relative electroelastic moduli with different parameter m_1 for $x_1/R = 1.2$, $m_4 = 0$. From the above definition, it is known that, if m_1 and m_4 are known, the values of m_2 and m_3 can easily be obtained. It is seen from Fig. 1 that the repulsive force acting on the piezoelectric screw dislocation increases with increasing relative shear modulus $c_{44}^{(1)}/c_{44}^{(2)}$. On the other hand, the attractive force will increase with increasing values of parameter m_1. The influence of the shear modulus of the inclusion on the image force will be very small when m_1 is taken to be a large

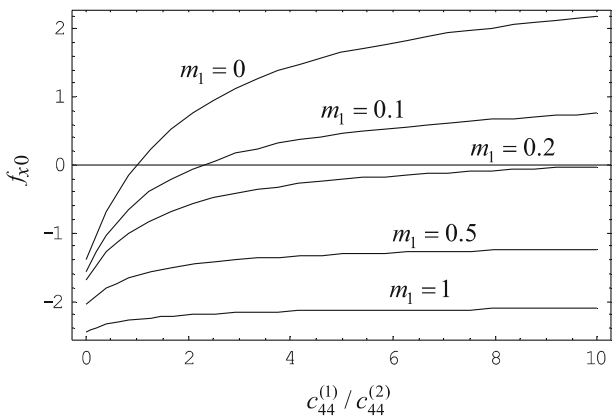

Fig. 1 f_{x0} versus $c_{44}^{(1)}/c_{44}^{(2)}$ for different values of $m_1 (e_{15}^{(1)} = e_{15}^{(2)}, \varepsilon_{11}^{(1)} = \varepsilon_{11}^{(2)}, x_1/R = 1.2, m_4 = 0)$

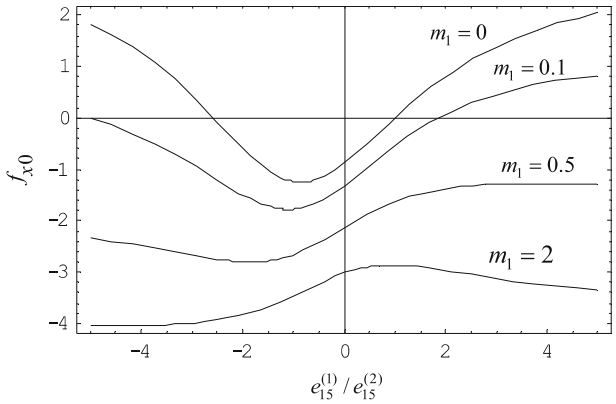

Fig. 2 f_{x0} versus $e_{15}^{(1)}/e_{15}^{(2)}$ for different values of $m_1 (c_{44}^{(1)} = c_{44}^{(2)}, \varepsilon_{11}^{(1)} = \varepsilon_{11}^{(2)}, x_1/R = 1.2, m_4 = 0)$

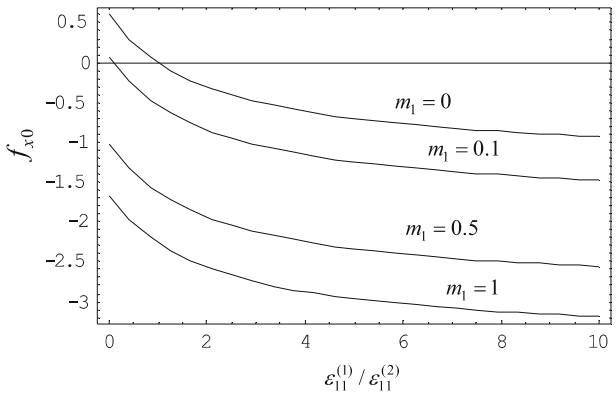

Fig. 3 $c_{44}^{(1)}/c_{44}^{(2)} = 0.1$ versus $\varepsilon_{11}^{(1)}/\varepsilon_{11}^{(2)}$ for different values of $m_1 (c_{44}^{(1)} = c_{44}^{(2)}, e_{15}^{(1)} = e_{15}^{(2)}, x_1/R = 1.2, m_4 = 0)$

value. Figure 2 shows that, if m_1 is taken to be a small value, the inclusion first attracts the piezoelectric screw dislocation, and then repels it with increasing absolute value of the ratio $e_{15}^{(1)}/e_{15}^{(2)}$. If m_1 is taken to be a large value, the inclusion will always attract the dislocation. By increasing the absolute value of the ratio $e_{15}^{(1)}/e_{15}^{(2)}$, the influence of the parameter m_1 will become more important and will obviously increase. It is observed from Fig. 3 that, if $m_1 = 0$, the inclusion will repel the dislocation when the value of the ratio $\varepsilon_{11}^{(1)}/\varepsilon_{11}^{(2)}$ is less than one. This rule is opposite to that given by either $c_{44}^{(1)}/c_{44}^{(2)}$ or $e_{15}^{(1)}/e_{15}^{(2)}$. Similarly, when the value of m_1 is large, regardless of the value of the ratio $\varepsilon_{11}^{(1)}/\varepsilon_{11}^{(2)}$, the inclusion will always attract the dislocation.

Figures 4 and 5 plot the variation of the normalized force f_{x0} with respect to the relative location of the dislocation x_1/R for different electroelastic property combinations for $m_1 = m_4 = 0.1$. It is found from Fig. 4 that there is no equilibrium position on the x-axis for soft inclusion and the inclusion always attracts the dislocation. When the inclusion is stiffer than the matrix (e.g., $c_{44}^{(1)}/c_{44}^{(2)} = 2$), the dislocation is first repelled then attracted by the inclusion when the dislocation approaches the inclusion from infinity. In this case, an unstable equilibrium position will be found on the x-axis. However, if the inclusion is very stiff (e.g., $c_{44}^{(1)}/c_{44}^{(2)} = 100$), the inclusion will always repel the dislocation and again no equilibrium position is available. Fig. 5 shows that, if $\varepsilon_{11}^{(1)}/\varepsilon_{11}^{(2)} \geq 1$, the inclusion always attracts the dislocation and no equilibrium position of the dislocation is available on the x-axis. On the other hand, if $\varepsilon_{11}^{(1)}/\varepsilon_{11}^{(2)} < 1$, the dislocation may be first attracted then repelled by the inclusion and an unstable equilibrium position may be available. However, when the value of the ratio $\varepsilon_{11}^{(1)}/\varepsilon_{11}^{(2)}$ is very small (e.g., $\varepsilon_{11}^{(1)}/\varepsilon_{11}^{(2)} = 0.1$), the inclusion always repels the dislocation and no equilibrium position is available on the x-axis.

Secondly, we utilize Eq. (14) together with Eq. (43) to illustrate the impact of various parameters on the image force when a single piezoelectric screw dislocation is located in the inclusion. The investigation of the dislocation located inside the inclusion may be helpful in estimating the energy levels involved for a dislocation to

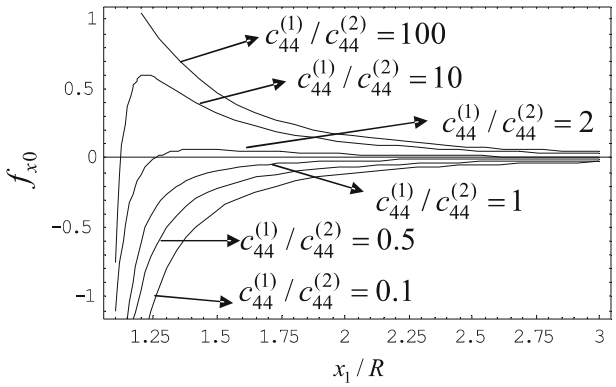

Fig. 4 f_{x0} versus x_1/R for different values of $c_{44}^{(1)}/c_{44}^{(2)}(e_{15}^{(1)}=e_{15}^{(2)}, \varepsilon_{11}^{(1)}=\varepsilon_{11}^{(2)}, m_1=m_4=0.1)$

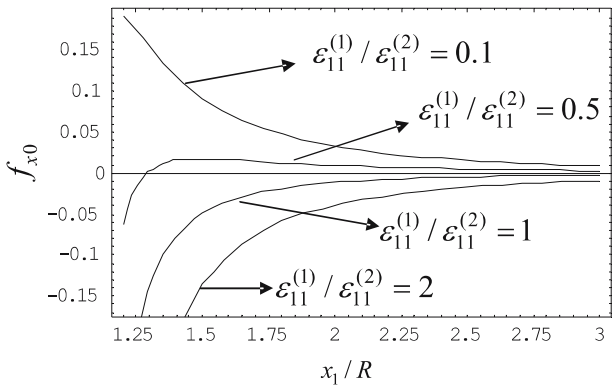

Fig. 5 f_{x0} versus x_1/R for different values of $\varepsilon_{11}^{(1)}/\varepsilon_{11}^{(2)}(c_{44}^{(1)}=c_{44}^{(2)}, e_{15}^{(1)}=e_{15}^{(2)}, m_1=m_4=0.1)$

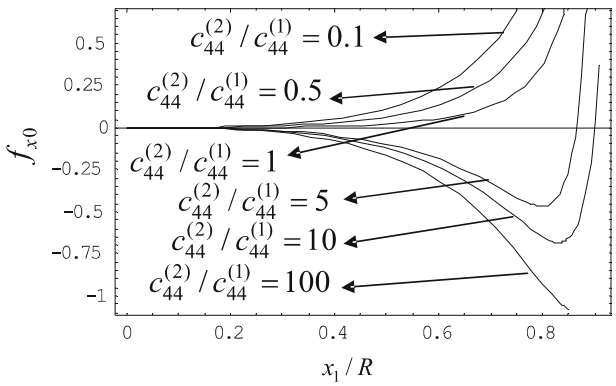

Fig. 6 f_{x0} versus x_1/R for different values of $c_{44}^{(2)}/c_{44}^{(1)}(e_{15}^{(2)}=e_{15}^{(1)}, \varepsilon_{11}^{(2)}=\varepsilon_{11}^{(1)}, m_1=m_4=0.1)$

cut the inclusion. Here, the piezoelectric screw dislocation vector $\mathbf{b}_1=\left[\, b_{z1}\ b_{\varphi 1}\,\right]^{\mathrm{T}}=\left[\, 1.0\times 10^{-9}m\ 1.0V\,\right]^{\mathrm{T}}$ is also used and the inclusion is taken to be PZT-5H with the electroelastic properties: $c_{44}^{(2)}=3.53\times 10^{10}\mathrm{N/m^2}$, $e_{15}^{(2)}=17.0\mathrm{C/m^2}$ and $\varepsilon_{11}^{(2)}=1.51\times 10^{-8}\mathrm{C^2/Nm^2}$[28]. Figures 6 and 7 show the variation of the normalized force f_{x0} with respect to the relative location of the dislocation x_1/R for different electroelastic property combinations. It is found from Fig. 6 that there is no equilibrium position of the dislocation on the x-axis for the case of a soft matrix and an imperfect interface. The dislocation will be attracted by the circular interface when the dislocation approaches the interface from center of the inclusion (original point). When the matrix is stiffer than the inclusion matrix (e.g., $c_{44}^{(2)}/c_{44}^{(1)}=5$), the dislocation is first repelled then attracted by the interface. In this case, an unstable equilibrium position will also be found on the x-axis inside the inclusion.

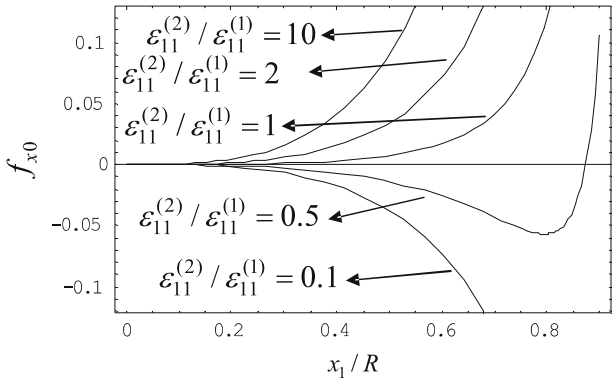

Fig. 7 f_{x0} versus x_1/R for different values of $\varepsilon_{11}^{(2)}/\varepsilon_{11}^{(1)}$ ($c_{44}^{(2)}=c_{44}^{(1)}$, $e_{15}^{(2)}=e_{15}^{(1)}$, $m_1=m_4=0.1$)

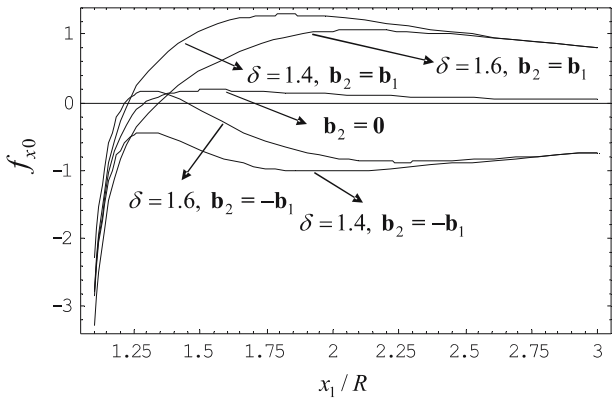

Fig. 8 f_{x0} versus x_1/R for different values of δ and $\mathbf{b}_2$($\alpha=30°$, $\mathbf{M}_1=5\mathbf{M}_2$, $m_1=m_4=1$)

However, if the matrix is very stiff (e.g., $c_{44}^{(2)}/c_{44}^{(1)}=100$), the interface will always repel the dislocation and again no equilibrium position is available. It is seen from Fig. 7 that, if $\varepsilon_{11}^{(2)}/\varepsilon_{11}^{(1)}\geq 1$, the interface always attracts the dislocation as the dislocation nears the interface. On the other hand, if $\varepsilon_{11}^{(2)}/\varepsilon_{11}^{(1)}<1$, the dislocation may be first repelled then attracted by the interface and an unstable equilibrium position may be available. However, when the value of the ratio $\varepsilon_{11}^{(2)}/\varepsilon_{11}^{(1)}$ is very small (e.g., $\varepsilon_{11}^{(2)}/\varepsilon_{11}^{(1)}=0.1$), the interface always repels the dislocation and no equilibrium position is available on the x-axis.

In the following, the effect of a closer parallel screw dislocations will be studied. Consider the case that two parallel piezoelectric screw dislocations $\mathbf{b}_1$ and $\mathbf{b}_2$ are located at the points $z_1(z_1=x_1)$ and $z_2=(z_2=re^{\mathrm{i}\alpha})$ in the matrix, respectively. The piezoelectric matrix material is also taken to be PZT-5H. The relative location of the dislocation z_2 relative to the inclusion is defined as $\delta=r/R$. The normalized image force f_{x0} with different values of δ and $\mathbf{b}_2$ as a function of x_1/R is depicted in Fig. 8 for $\theta=30°$, $\mathbf{M}_1=5\mathbf{M}_2$ and $m_1=m_4=1$. It can be seen that, when x_1/R reaches a critical value, the direction of the image force acting on the screw dislocation z_1 produced by the dislocation z_2 can be changed in the two cases $\mathbf{b}_2=\mathbf{b}_1$ and $\mathbf{b}_2=-\mathbf{b}_1$. For the case $\mathbf{b}_2=-\mathbf{b}_1$, if the two dislocations are close to one another, the unstable equilibrium point of the dislocation z_1 near the inclusion may disappear due to the effect of the nearby dislocation z_2. However, if the distance is larger, a new stable equilibrium point of the dislocation z_1 may be produced along the x-axis direction and there are two equilibrium points when the dislocation z_1 approaches the inclusion from infinity. On the other hand, for the case $\mathbf{b}_2=\mathbf{b}_1$, the number and stability of equilibrium points of the dislocation will not be altered, but the position of equilibrium point is variable to consider the effect of nearby dislocations. The normalized image force f_{x0} with various values of $\mathbf{b}_2$ and m_j as a function of θ is shown in Fig. 9 for $x_1/R=1.2$, and $\mathbf{M}_1=5\mathbf{M}_2$. Figure 9 indicates that the direction of the image force exerted on the dislocation z_1 produced by the dislocation z_2 will be altered when the absolute value of the angle α reaches a critical value for the two cases $\mathbf{b}_2=\mathbf{b}_1$ and $\mathbf{b}_2=-\mathbf{b}_1$. The effect of the dislocation z_2 on the image force acting on the dislocation z_1 is very obvious when two screw dislocations are both located on the x-axis. The direction of the

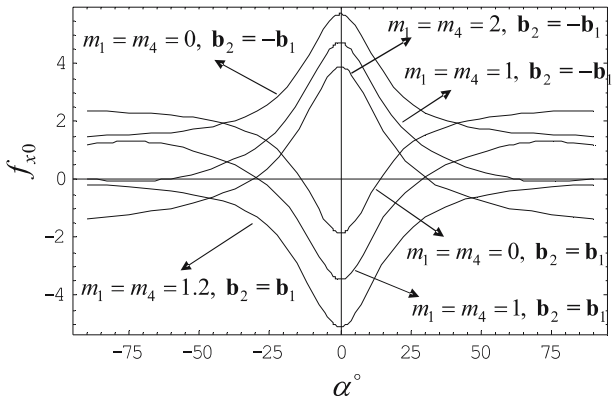

Fig. 9 f_{x0} versus α° for different values of m_j and $\mathbf{b}_2(x_1/R = 1.2, \mathbf{M}_1 = 5\mathbf{M}_2, \delta = 1.6)$

total image force exerted on the dislocation z_1 will be altered when the absolute value of the angle α reaches a critical value, considering the effect of the interface imperfection for the case $\mathbf{b}_2 = -\mathbf{b}_1$. A new equilibrium position of the dislocation z_1 along the x-axis direction may be produced. However, for the case $\mathbf{b}_2 = \mathbf{b}_1$, the original equilibrium position of dislocation z_1 along the x-axis direction may disappear due to the effect of the interface imperfection.

5 Conclusions

The problem of the interaction between multiple piezoelectric screw dislocations, located inside either the inclusion or the matrix, and a circular inclusion with an imperfect interface under remote uniform anti-plane shear stresses and in-plane electric fields is studied. By the use of the complex-variable method, the explicit solutions for the electroelastic fields and image forces exerted on the piezoelectric screw dislocations are calculated. The impact of interface imperfection and material electroelastic mismatch as well as the nearby parallel screw dislocations on the image force and the equilibrium position of the appointed piezoelectric screw dislocation are examined and discussed in detail. The results show that the attractive force exerted on the dislocation produced by the imperfect interface increases with the increment of the degree of interface imperfection. If the degree of interface imperfection is biggish, the influence of material electroelastic mismatch on the image force and the equilibrium position of the dislocation is small. The equilibrium positions of the appointed piezoelectric screw dislocation are strongly influenced by nearby parallel screw dislocations. The original equilibrium positions of the dislocation may disappear and the new equilibrium positions can be produced, considering the effect of the nearby dislocations.

Acknowledgments The authors appreciate support by the National Natural Science Foundation of China (10472030). In addition, authors are grateful to the anonymous reviewers for their valuable comments and suggestions.

References

1. Dundurs, J., Mura, T.: Interaction between an edge dislocation and a circular inclusion. J. Mech. Phys. Solids **12**, 177–189 (1964)
2. Smith, E.: The interaction between dislocation and inhomogeneities-1. Int. J. Eng. Sci. **6**, 129–143 (1968)
3. Stagni, L., Lizzio, R.: Shape effects in the interaction between an edge dislocation and an elliptic inhomogeneity. Appl. Phys. A **30**, 217–221 (1983)
4. Qaissaunee, M.T., Santare, M.H.: Edge dislocation interaction with an elliptical inclusion surrounding by an interfacial zone. Q. J. Mech. Appl. Math. **48**, 465–482 (1995)
5. Xiao, Z.M., Chen, B.J.: A screw dislocation interacting with a coated fiber. Mech. Mater. **37**, 485–494 (2000)
6. Xiao, Z.M., Chen, B.J.: Stress analysis for a Zener–Stroh crack interacting with a coated inclusion. Int. J. Solids Struct. **38**, 5007–5018 (2001)
7. Churchman, A.M., Korsunsky, A.M., Hills, D.A.: The edge dislocation in a three-quarter plane. Part II Application to an edge crack. Euro. J. Mech. A/Solids **25**, 389–396 (2006)
8. Kattis, M.A., Providas, E., Kalamkarov, A.L.: Two-phone potentials in the analysis of smart composites having piezoelectric components.. Composites Pt. B **29**(1), 9–14 (1998)

9. Meguid, S.A., Deng, W.: Electro–elastic interaction between a screw dislocation and elliptical inhomogeneity in piezoelectric materials. Int. J. Solids Struct. **35**, 1467–1482 (1998)
10. Huang, Z., Kuang, Z.B.: Dislocation inside a piezoelectric media with an elliptical inhomogeneity. Int. J. Solids Struct. **38**, 8459–8480 (2001)
11. Liu, Y.W., Fang, Q.H., Jiang, C.P.: A piezoelectric screw dislocation interacting with an interphase layer between a circular inclusion and the matrix. Int. J. Solids Struct. **41**, 3255–327 (2004)
12. Xiao, Z.M., Yan, J., Chen, B.J.: Electro-elastic stress analysis for a screw dislocation interacting with a coated inclusion in piezoelectric solid. Acta Mech. **1**(27), 237–249 (2004)
13. Hashin, Z.: The spherical inclusion with imperfect interface. J. Appl. Mech. **58**, 444–449 (1991)
14. Ru, C.P., Schiavone, P.: A circular inclusion with circumferentially inhomogeneous interface in antiplane shear. Proc. R. Soc. Lond. A. **453**, 2551–2572 (1997)
15. FanH.; Wang, G.F.: Screw dislocation interacting with imperfect interface. Mech. Mater. **35**, 943–953 (2003)
16. Sudak, L.J.: On the interaction between a dislocation and a circular inhomogeneity with imperfect interface in antiplane shear. Mech. Res. Commun. **30**, 53–59 (2003)
17. Sudak, L.J.: between a screw dislocation and a three-phase circular inhomogeneity with imperfect interface. Math. Mech. Solids **8**, 171–188 (2003)
18. Wang, X.: Interaction between an edge dislocation and a circular inclusion with an inhomgeneously imperfect interface. Mech. Res. Commun. **33**, 17–25 (2006)
19. Fan, H., Sze, K.Y.: An micro-mechanics model for imperfect interface in dielectric materials. Mech. Mater. **33**, 363–370 (2001)
20. Pak, Y.E.: Circular inclusion problem in antiplane piezoelectricity. Int. J. Solids Struct. **29**, 2403–2419 (1992)
21. Pak, Y.E.: Force on the piezoelectric screw dislocation. J. Appl. Mech. **57**, 863–869 (1990)
22. Barnett, D.M., Lothe, J.: Dislocations and line charges in anisotropic piezoelectric insulators. Phys. Status Solid (B) **67**, 105–111 (1975)
23. Chen, B.J., Xiao, Z.M., Liew, K.M.: On the interaction between a semi-infinite anti-crack and a screw dislocation in piezoelectric solid. Int. J. Solids Struct. **39**, 1505–1513 (2002)
24. Muskhelishvili, N.L.: Some Basic Problems of Mathematical Theory of Elasticity. Noordhoff, Leyden (1975)
25. Gao, C.F., Kessler, H., Balke, H.: Green's functions for anti-plane deformations of a circular arc-crack at the interface of piezoelectric materials. Arch. Appl. Mech. **73**, 467–480 (2003)
26. Hirth, J.P., Lothe, J.: Theory of Dislocations, 2nd edn. Wiley, New York (1982)
27. Lee, S.: The image force on the screw dislocation around a crack of finite size. Eng. Fract. Mech. **27**, 539–545 (1987)
28. Lee, K.Y., Lee, W.G., Pak, Y.E.: Interaction between a semi-infinite crack and a screw dislocation in a piezoelectric material. J. Appl. Mech. **67**, 165–170 (2000)